

## Values of Mineral Modulus of Clay

Manika Prasad, Ronny Hofmann, Mike Batzle, Colorado School of Mines; M. Kopycinska-Müller, U. Rabe, and W. Arnold, Fraunhofer Institute for Nondestructive Testing, IZFP, Saarbrücken

### Summary

Seismic wave propagation in geological formations is altered by the presence of clay minerals. Knowledge about the elastic properties of clay is therefore essential for the interpretation and modeling of the seismic response of clay-bearing formations. However, due to the layered structure of clay, it is very difficult to investigate its elastic properties. We measured elastic properties of clay using atomic force acoustic microscopy (AFAM). The forces applied during the experiments were not higher than 50 nN. The adhesion forces were measured from the pull-off forces and included into our calculations by means of the Derjaguin-Mueller-Toporov model for contact mechanics. The obtained values of the elastic modulus for clay varied from 10 to 17 GPa depending on various parameters that describe the dynamics of a vibrating beam.

### Introduction

Clay is one of the most common sedimentary minerals on Earth. Seismic wave propagation in geological formations is altered by the presence of clay minerals. When the clay is load-bearing, it forms a weak link between larger and stronger components of various geological structures. Fig. 1 shows a comparison between scanning electron (SEM), atomic force (AFM), and scanning acoustic microscopy (SAM) images of a sandstone. Fig. 1a (from du Bernard et al., 2003) illustrates location of clay particles around quartz grains. Although, topography changes were too large (Fig. 1b) to make quantitative measurements on such samples, SAM images (Fig. 1c) do show lower impedance for clay as compared to quartz. Presence of clay alters the elastic and plastic behavior of the composite material significantly. And so, knowledge about the elastic properties of clay is essential for interpreting and modeling the seismic response of clay-bearing formations. However, the layered structure of clay makes this a challenging measurement. There are many problems associated with elastic properties measurements of clay minerals with standard pulse transmission techniques. Clay “booklets” usually consist of many layers with thicknesses in the range of few nm. Until now, estimates of single crystal elastic properties have been either theoretical (Katahara, 1996), or based on extrapolations from measurements on clay-epoxy mixtures (Wang et al., 2001). For these reasons, there is a large discrepancy in the values of elastic modulus of clay minerals (Table 1).

Table 1. Values of Bulk modulus of Kaolinite from various sources. 1 = Vanorio et al., 2001, 2 = Wang et al., 2001, 3 = Katahara, 1996.

Sample	1		2		3	
	K	$\mu$	K	$\mu$	K	$\mu$
Kaolinite	10	5.0	47.9	19.7	55.5	31.8

In the following, we present measurements of elastic properties of clay minerals (dickite) and mica particles using atomic force acoustic microscopy (AFAM). This technique is a dynamic enhancement of the atomic force microscope (AFM) technique and its principles are described in details elsewhere (Rabe et al., 1996, 1998, 2000). Sample preparation is explained in Prasad et al. (2002).

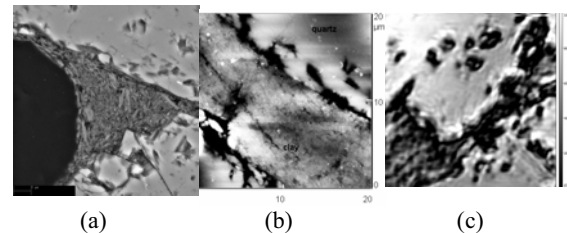


Figure 1: Comparison between (a) SEM, (b) AFM, and (c) SAM images of a contact zone in a thin section of a sandstone with clay cements. 1a shows the alignment of the clay around quartz grains in the contact. However, topographic effects dominate (1b). The SAM image shows that clays have lower impedance (darker color) than the quartz (lighter color).

### Topography Measurements

Topography images were first obtained in contact mode using a triangular cantilever with a low spring constant. The imaged structures were not stable and it was observed that scanning the sample surface in the contact mode actually damaged the sample. Therefore, tapping mode AFM was considered more suitable for imaging this material. Tapping mode not only ensures higher lateral resolution but also protects the sample structures better. The AFM topography imaging result are presented in Fig. 2, which shows a typical clay booklet structure. One can clearly see a stack of seven thin layers, each with a thickness less than 1 nm (as given by Velde, 1992). The image size was  $1 \mu\text{m} \times 1 \mu\text{m}$  with a height scale of about 10 nm.

## Values of Mineral Modulus of Clay

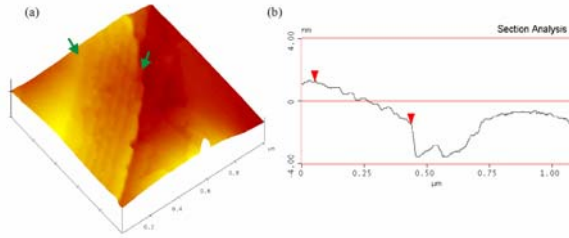


Figure 2: AFM topography image of dickite (a). The arrows mark location of the cross-section shown in (b). The size of the image is  $1 \mu\text{m} \times 1 \mu\text{m}$ . Here typical clay booklets can be observed. As can be seen in (b) the height scale is about 10 nm. As the vertical distance between the two marked points is about 3 nm it can be concluded that the thickness of the clay layers is less than 1 nm.

### AFAM Resonance Spectra

Preliminary results showed, however, that the clay sample was much more compliant than the fused quartz sample. In order to improve the accuracy of the measured values, additional measurements were made on polystyrene that has an elastic modulus lower than that of clay. Mica particles were mingled with the clay. Since the AFAM measurements were made at random locations, occasionally the tip came into contact with mica instead of clay. The properties of mica are closer to those of fused quartz than to clay, so it was possible to identify and interpret the measurements on mica. Fig. 3 shows examples of normalized contact-resonance spectra measured on clay, polystyrene, mica and fused quartz. Contact-resonance frequencies measured on clay are slightly higher than the frequencies detected on polystyrene and lower than the contact-resonance frequencies measured on mica and fused quartz. This difference is greater for the second contact-resonance frequencies. The relative difference in the contact resonance frequencies for different materials depends on the mode of the cantilever vibration (Turner et al, 1997).

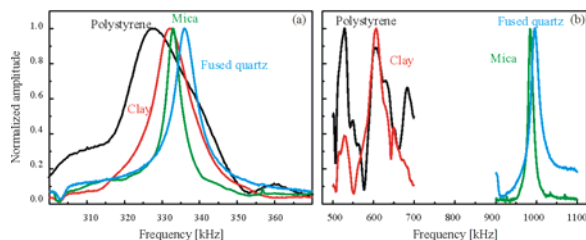


Figure 3: Contact-resonance spectra measured on polystyrene, clay, mica, and fused quartz. The relative frequency of the contact-resonance peaks implies that the indentation modulus of clay lies between that of polystyrene and that of mica and fused quartz. The differences are minimal for the first contact-resonance frequency (a) but are much larger for the second contact-resonance frequency (b). The spectra shown here were normalized to

emphasize the differences in the position of the contact resonance frequency (from Prasad et al., 2002).

The AFAM spectra were measured in sweep mode. Twenty-five spectra were measured at each location for each static load. The curves presented in Fig. 3 were obtained by averaging the 25 measured spectra. All of the average values of the first and the second contact resonance frequencies are shown in Fig. 4. The error bars represent the standard deviation of 25 measurements. In most cases, the standard deviation is so small, that the error bars are actually smaller than the size of the symbol that represents the value of the resonance frequency. Large error bars correspond to measurements during which the contact resonance frequency changed, probably due to the sliding of the booklets. Figure 4 shows that in almost all cases, the measured spectra behaved like those in Fig. 3. The differences between the values of the first contact resonance frequency measured on the fused quartz and the clay sample are small. In a few cases, the first resonance frequency measured on the clay sample is actually higher than the resonance frequency measured on the fused quartz sample. Such behavior was previously observed for these types of AFM cantilever (Kopycinska-Mueller, 2005). The second contact resonance frequency measured on the clay sample is lower than the corresponding frequency for the fused quartz sample by about 400 kHz.

### Results

The resonance frequencies (Fig. 4) were used to determine the tip position parameter  $L1/L$  and then to calculate the local tip-sample contact stiffness  $k^*$  (for example, Rabe et al., 1996, 2000, 2002). The optimum value of  $L1/L$  was found to be 0.873. One can calculate an error value  $\Delta k^*$  defined as a difference of the stiffness calculated for the two modes separately at the determined value of  $L1/L$   $\Delta k^* = 100\% \times 2(k^*(f1)-k^*(f2))/(k^*(f1)+k^*(f2))$ . Smaller the value of  $\Delta k^*$  better the agreement between the measured contact resonance frequencies and the dynamic beam model. The results obtained for  $k^*$  and  $\Delta k^*$  (Fig. 5) show that the values of  $k^*$  calculated for fused quartz are twice as large as  $k^*$  values obtained for the clay sample. It can also be noticed that there is a significant difference in  $\Delta k^*$  calculated for the clay and for the fused quartz sample. For the clay sample, the difference between the values of  $k^*$  calculated for the first and second modes is smaller than 20 %. An equivalent calculation performed for the fused quartz sample yielded  $\Delta k^* = 110 \%$ . The value of  $L1/L$  determined was not optimal for all of the measured contact-resonance frequencies.  $L1/L = 0.909$  is the value obtained for the resonance frequencies measured on the fused quartz sample only. Because more resonance frequencies were measured on the clay sample than on the fused quartz sample, the calculated value of  $L1/L$  will be weighted

Values of Mineral Modulus of Clay

toward the values of the frequencies measured on the clay sample. These results suggest that the tip-position  $L_1/L$  relates not only to the physical tip position but also to the elastic properties of the sample and to the measured contact mode. As the first contact resonance frequency measured on fused quartz was pinned, there is a strong suspicion that the ratio of the vertical and lateral forces acting between the tip and the sample for the first mode is different from the same ratio for the second mode. This may alter the results of the calculation, as the different dynamic of the pinned modes is not included into analytical model of the vibrating beam. Note that all inconsistencies in contact stiffness evaluation are assigned to  $L_1/L$ . Future work could involve modifying the physical model to also account for the eigenmodes of the cantilever.

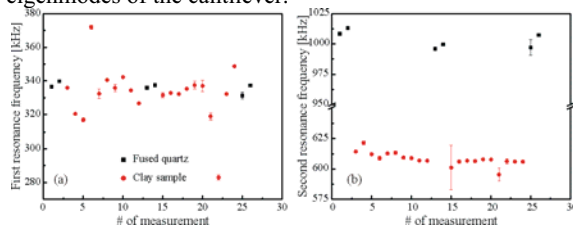


Figure 4: (a) First and (b) second contact-resonance frequency measured on fused quartz (■) and clay (●). Each resonance frequency was measured at static loads of 30 nN and 45 nN. The spectra were measured in sweep mode. Results presented here are the average values of 25 measured resonance frequencies. In some cases, the contact-resonance frequency changed significantly during the measurement giving rise to large standard deviations. Note the break in y-scale between 650 and 950 kHz in (b).

The tip position parameter has a strong impact on the value calculated for the local tip-sample contact stiffness. Table 2 compares the values of  $k^*$  calculated for the fused quartz sample using  $L_1/L = 0.873$  and  $0.909$ . As can be seen in Table 1, the calculated values of  $k^*$  differ significantly when different values of  $L_1/L$  are assumed. The values of  $k^*$  obtained for  $L_1/L = 0.909$  are about 50% higher than those obtained for  $L_1/L = 0.873$ . The values of  $k^*$  used for the reference sample affect the calculated elastic properties of the clay sample. For example, the average value of the indentation modulus  $M_{clay}$  calculated for the clay sample is  $16.9 \text{ GPa} \pm 6.3 \text{ GPa}$  if the values of  $k^*$  for quartz with  $L_1/L = 0.873$  are used. However, when the values of  $k^*$  for quartz calculated for  $L_1/L = 0.909$  are used, the average value of  $M_{clay} = 9.9 \text{ GPa} \pm 3.3 \text{ GPa}$ . Taking into account the additional reference measurement on the polystyrene sample for which  $M$  is approximately  $3.8 \text{ GPa}$ , the result  $M = 9.9 \text{ GPa} \pm 3.3 \text{ GPa}$  is likely to be closer to the real properties of clay. Currently, there are no other measurements of the elastic properties of clay for comparison. Theoretical estimates available (Berge and Berryman, 1995) yield a value for the Young’s modulus of clay of  $10\text{-}12 \text{ GPa}$ .

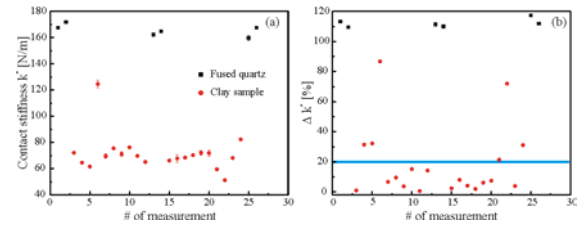


Figure 5:  $k^*$  calculated from the resonance frequencies measured on the fused quartz and clay samples at a fixed  $L_1/L = 0.873$ . (b)  $\Delta k^*$  in the values of  $k^*(f_1)$  and  $k^*(f_2)$  calculated for this value of  $L_1/L$ .  $\Delta k^*$  varies strongly depending on the elastic properties of the sample. For the clay sample,  $\Delta k^*$  is less than 20 % in almost all cases. For the fused quartz sample, however,  $\Delta k^*$  is greater than 100 %, indicating that the chosen value of  $L_1/L$  is not optimal.

Table 2. Impact of the tip-position parameter  $L_1/L$  on the tip-sample contact stiffness  $k^*$ , calculated for the measurements on the fused quartz sample. The values of  $k^*$  calculated using a tip-position determined from the entire set of measurements ( $L_1/L = 0.873$ ) are significantly lower than the values of  $k^*$  calculated at tip position of  $L_1/L = 0.9090$ , the value determined from the fused quartz measurements only.

M/s #	Static load [nN]	$L_1/L = 0.873$		$L_1/L = 0.909$	
		$k^*$ [N/m]	$\Delta k^*$ [%]	$k^*$ [N/m]	$\Delta k^*$ [%]
1	30	167.57	113.21	234.42	76.18
	45	171.89	109.59	246.24	70.02
2	30	162.37	111.36	222.36	71.51
	45	164.86	110.00	228.73	69.25
3	30	159.79	117.50	214.39	83.59
	45	167.65	111.95	234.97	73.69

Conclusions and Future Work

The Young’s modulus for clay measured with AFAM lies between  $10 - 15 \text{ GPa}$ . The measurement uncertainty of our measurements is estimated at  $\pm 8 \text{ GPa}$ . These results have been very encouraging. For the future we plan to make measurements as functions of varying water content by drying and baking of the clay minerals and by varying humidity in the sample through a controlled environmental chamber (Hurley and Turner, 2004).

References

Berge, P. A. and Berryman, J. G., 1995, Realizability of Negative Pore Compressibility in Poroelastic Composites, Journal of Applied Mechanics 62, 1053-1062.

Du Bernard, X., Prasad, M., Reinstaedtler, M., 2003, The effect of cementation on the seismic properties of sandstones, Proc. Int. Symp. Acoustical Imaging, Eds. W. Arnold and S. Hirsekorn, 27, 399-405.

### Values of Mineral Modulus of Clay

Hurley, D.C., and Turner, J. A., 2004, *J. Appl. Phys.* 95, p. 2403.

Katahara, K. W., Clay mineral elastic Properties, SEG Expanded Abstracts, Paper RP1.4, 1996.

Kopycinska-Mueller, M., 2005, On the elastic properties of nanocrystalline materials and the determination of elastic properties on a nanoscale using the atomic force acoustic microscopy technique: PhD thesis, Technical Faculty of Saarland University, Saarbruecken (in preparation).

Prasad, M., Kopycinska, M., Rabe, U., and Arnold, W., 2002, Measurement of Young's modulus of clay minerals using Atomic Force Acoustic Microscopy, *Geophysical Research Letters*, Vol. 29, #8, 13-1 – 13-4.

Rabe, U., Janser, K., and Arnold, W., 1996, Vibrations of free and surface-coupled atomic force microscopy cantilevers: theory and experiment, *Rev. Sci. Instrum.* 67, p. 3281-3293.

Rabe, U., Turner, J., and Arnold, W., 1998 Analysis of the High-Frequency Response of Atomic Force Microscope Cantilevers, *Appl. Phys. A* 66, S277- S282.

Rabe, U., Amelio, S., Kester, E., Scherer, V., Hirsekorn, S., and Arnold, W., 2000, Quantitative Determination of Contact Stiffness Using Atomic Force Acoustic Microscopy *Ultrasonics* 38, 430-437.

Rabe, U., Amelio, S., Kopycinska, M., Hirsekorn, S., Kempf, M., Göken, M., and Arnold, W., 2002, Imaging and Measurement of Local Mechanical Material Properties by Atomic Force Acoustic Microscopy, *Surf. Interface Anal.* 33, p. 65.-70

Turner, J., Hirsekorn, S., Rabe, U., and Arnold, W., 1997, High-Frequency Response of Atomic-Force Microscope Cantilevers, *J. Appl. Phys.* 82, 966-970.

Velde, B., 1992, Introduction to clay minerals, chemistry, origins, uses and environmental significance, Chapman and Hall, London, United Kingdom.

Wang, Z., Wang, H., and Cates, M. E., Effective Elastic Properties of Solid Clays, *Geophysics* 66, 428-440, 2001.

#### Acknowledgements

We acknowledge the support of the sponsors Colorado School of Mines - University of Houston Fluids / DHI Consortium and the National Science Foundation (Grant No. EAR 0074330).

## EDITED REFERENCES

Note: This reference list is a copy-edited version of the reference list submitted by the author. Reference lists for the 2005 SEG Technical Program Expanded Abstracts have been copy edited so that references provided with the online metadata for each paper will achieve a high degree of linking to cited sources that appear on the Web.

### Values of Mineral Modulus of Clay

#### REFERENCES

- Berge, P. A., and J. G. Berryman, 1995, Realizability of negative pore compressibility in poroelastic composites: *Journal of Applied Mechanics*, **62**, 1053-1062.
- Du Bernard, X., M. Prasad, and M. Reinstaedtler, 2003, The effect of cementation on the seismic properties of sandstones, in W. Arnold and S. Hirsekorn, eds., *Proceedings of the International Symposium on Acoustical Imaging*, **27**, 399-405.
- Hurley, D. C., and J. A. Turner, 2004, *Journal of Applied Physics*, **95**, 2403.
- Katahara, K. W., 1996, Clay mineral elastic properties: 66th Annual International Meeting, SEG, Expanded Abstracts, 1691-1694.
- Kopycinska-Mueller, M., 2005, On the elastic properties of nanocrystalline materials and the determination of elastic properties on a nanoscale using the atomic force acoustic microscopy technique: Ph.D. thesis, Technical Faculty of Saarland University, Saarbruecken (in preparation).
- Prasad, M., M. Kopycinska, U. Rabe, and W. Arnold, 2002, Measurement of Young's modulus of clay minerals using Atomic Force Acoustic Microscopy: *Geophysical Research Letters*, **29**, no. 8, 13-1 – 13-4.
- Rabe, U., K. Janser, and W. Arnold, 1996, Vibrations of free and surface-coupled atomic force microscopy cantilevers: theory and experiment: *Review of Scientific Instruments*, **67**, 3281-3293.
- Rabe, U., J. Turner, and W. Arnold, 1998, Analysis of the high-frequency response of atomic force microscope cantilevers: *Applied Physics A*, **66**, S277- S282.
- Rabe, U., S. Amelio, E. Kester, V. Scherer, S. Hirsekorn, and W. Arnold, 2000, Quantitative determination of contact stiffness using atomic force acoustic microscopy: *Ultrasonics*, **38**, 430-437.
- Rabe, U., S. Amelio, M. Kopycinska, S. Hirsekorn, M. Kempf, M. Göken, and W. Arnold, 2002, Imaging and measurement of local mechanical material properties by atomic force acoustic microscopy: *Surface and Interface Analysis*, **33**, 65-70.
- Turner, J., S. Hirsekorn, U. Rabe, and W. Arnold, 1997, High-frequency response of atomic-force microscope cantilevers: *Journal of Applied Physics*, **82**, 966-970.
- Velde, B., 1992, *Introduction to clay minerals, chemistry, origins, uses and environmental significance*: Chapman and Hall.
- Wang, Z., H. Wang, and M. E. Cates, Effective elastic properties of solid clays: *Geophysics*, **66**, 428-440, 2001.